Normal Modes of 2D Finite Clusters in Complex Plasmas

A. Melzer, M. Klindworth, and A. Piel

Institut für Experimentelle und Angewandte Physik, Christian-Albrechts-Universität Kiel, 24098 Kiel, Germany

(Received 29 May 2001; published 24 August 2001)

Finite clusters with a small number of charged particles immersed in a complex-plasma environment have been investigated experimentally. Finite clusters in complex plasmas are shown to be a unique system for the excitation and observation of normal modes in bounded charged-particle systems. In systems of 3, 4, and 7 particles, normal-mode oscillations have been excited and from the frequencies of the different modes the key parameters, particle charge, and the screening strength have been derived. This method is proposed to be applied in future microgravity experiments.

DOI: 10.1103/PhysRevLett.87.115002 PACS numbers: 52.27.Lw, 36.40.Sx

Finite Coulomb clusters are systems of a small number of charged particles, $N = 1$ to 100, confined by an external potential. Such charged-particle systems are a topic of high interest to various fields of physics starting with theoretical investigations related to Thomson's classical atom model [1]. Three-dimensional (3D) Coulomb clusters are found for ions in Paul and Penning traps [2,3]. 2D Coulomb clusters have experimentally been realized as electrons on liquid helium [4], in quantum dots [5], or in colloidal suspensions with macroscopic particles [6,7]. Very recently, 2D Coulomb clusters have also been prepared and studied in laboratory complex plasmas [8,9] and 3D clusters are expected in future experiments under microgravity. It will be shown here that finite clusters in complex plasmas are a unique paradigm for the excitation, observation, and quantitative analysis of weakly damped normal modes of bounded charged-particle systems in general to reveal the key cluster parameters. The excitation of normal modes will be an indispensable diagnostic for future experiments under microgravity, where the resonance method [10] is not applicable.

Because of the small number of particles involved clusters are especially intriguing for detailed theoretical studies and simulations. Cluster structures [11,12] as well as phase transitions, eigenmodes, and energy spectra have been calculated [11,13,14].

Typical laboratory experiments on complex plasmas are performed in parallel plate rf discharges. Monodisperse microspheres are immersed in the gaseous discharge plasma of electrons, ions, and neutrals. Since the electrons are much more mobile than the ions, the microspheres attain a high negative charge of the order of several thousand elementary charges [10]. The particles are trapped in the space charge sheath above the lower electrode where the electric field force levitates the microspheres against the gravitational force. Because of this force balance the particles arrange in a horizontally extended 2D structure. Under an additional horizontal confinement the particles arrange in 2D finite clusters.

The structure and dynamics of finite clusters is determined by the interplay of potential energy in the confining well and the mutual Coulomb repulsion of the microspheres. The electrostatic interaction in the horizontal plane is usually described by a screened Coulomb (Debye-Hückel or Yukawa) potential, as confirmed by recent experiments on compressional waves [15,16] or by the analysis of binary collisions [17]:

$$\phi(r) = \frac{Ze}{4\pi\epsilon_0 r}\exp\left(-\frac{r}{\lambda_D}\right), \tag{1}$$

where Z is the charge number of the microspheres and λ_D is the screening length due to shielding by the ambient plasma electrons and ions. The total energy of the system of N particles is then given by the sum of their potential and electrostatic energy

$$E = \frac{1}{2}m\omega_0^2\sum_{i=1}^{N} r_i^2 + \frac{Z^2e^2}{4\pi\epsilon_0}\sum_{i>j}^{N}\frac{1}{r_{ij}}\exp\left(-\frac{r_{ij}}{\lambda_D}\right). \tag{2}$$

Here, ω_0^2 is a measure of the strength of the horizontal parabolic confinement, r_i is the distance of the ith particle from the center of the potential well, and r_{ij} is the relative distance between particles i and j.

By normalizing the energy to E_0 and the distances to r_0 with

$$E_0 = \left[\frac{m\omega_0^2}{2}\left(\frac{Z^2e^2}{4\pi\epsilon_0}\right)^2\right]^{1/3}, \qquad r_0 = \left[\frac{2}{m\omega_0^2}\frac{Z^2e^2}{4\pi\epsilon_0}\right]^{1/3} \tag{3}$$

the total energy can be written conveniently as [11]

$$E = \sum_{i=1}^{N} r_i^2 + \sum_{i>j}^{N}\frac{\exp(-r_{ij}\kappa)}{r_{ij}}, \tag{4}$$

where E and r_i are now normalized quantities and

$$\kappa = \frac{r_0}{\lambda_D} \tag{5}$$

is the screening strength.

2D clusters of N particles can exhibit a number of normal modes. The mode frequencies are obtained from the eigenvalues and the particle motion results from the eigenvectors of the dynamical matrix [13,14]

$$E_{\alpha\beta,ij} = \frac{\partial^2 E}{\partial r_{\alpha,i}\partial r_{\beta,j}} \tag{6}$$

with α and $\beta = x, y$ and $r_{\alpha,i}$ denotes the x or y coordinate of the ith particle.

For the case of pure Coulomb interaction ($\kappa = 0$) there are three normal modes that are independent of the particle number N [13]: (i) $\omega = 0$ for the rotation of the entire cluster around the center of the confinement, (ii) $\omega = \omega_0$ (twofold degenerate) oscillation of the center-of-mass of the cluster in the horizontal potential well, and (iii) $\omega = \sqrt{3}\,\omega_0$ corresponds to a coherent radial oscillation of all particles (breathing mode). For screened interaction ($\kappa \neq 0$), the frequency of the first two modes is unaffected since they do not involve a relative particle motion. In contrast, the frequency of the breathing mode becomes dependent on κ and, weakly, on the particle number N.

In the experiments, we will focus on these three modes and a fourth one, where neighboring particles oscillate radially in the opposite direction (antisymmetric mode), see below. The frequency of that mode also depends on particle number and screening strength. We will present measurements that allow a simultaneous determination of these eigenmodes in 2D clusters in a complex plasma with $N = 3$, 4, and 7 particles. From the frequencies of the different modes the defining parameters of finite clusters, the confinement potential ω_0, screening strength κ, and the particle charge Z, are measured.

The experiments have been performed in a capacitively coupled parallel plate rf discharge operated in argon at a quite low gas pressure of 1.6 Pa to ensure weak damping. The lower electrode was operated at 13.56 MHz and 9 W forward and 1 W reflected power with a peak-to-peak voltage of $V_{pp} = 37$ V. The upper electrode and the discharge vessel were grounded (see Fig. 1a). Melamine/formaldehyde microspheres of 9.47 μm diameter ($m = 6.73 \times 10^{-13}$ kg) are dropped into the plasma and form a 2D finite Coulomb cluster above the lower electrode. The horizontal confinement for the particles is realized by a shallow circular parabolic trough in the electrode (see Fig. 1a). The 2D Coulomb clusters of microspheres are illuminated by a laser sheet and are recorded from the top with a charge-coupled device (CCD) video camera.

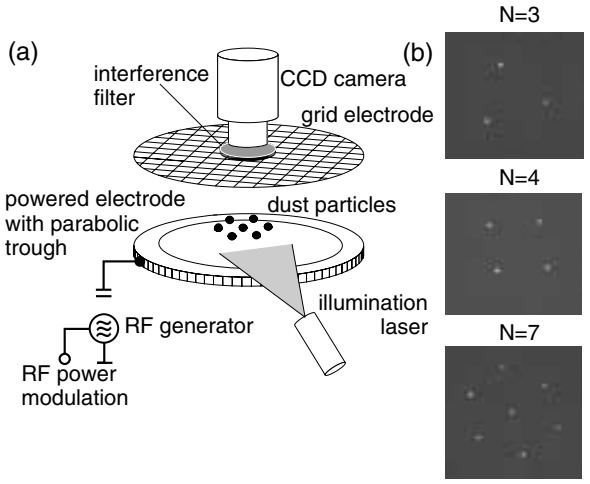

FIG. 1. (a) Scheme of the experimental setup; (b) images of the equilibrium of the clusters with $N = 3$, 4, and 7 particles.

The normal modes are excited by a pulse modulation of the rf electrode voltage. Therefore, the output of the rf generator is reduced to a lower value ($V_{pp} = 27$ V) for 30 ms and, after that, increased to the constant value of 9 W again. During the low rf power pulse the cluster shrinks in size and is restored to the original size again thus starting oscillations in the cluster. The oscillations are a superposition of the normal modes of the cluster. Vertical oscillations in the sheath potential that are also excited have been neglected due to the fact that the vertical amplitude is smaller than the horizontal and that it is a coherent oscillation of all particles.

The different normal modes of the cluster are then identified from the trajectories of the particles according to the eigenvectors of the modes. First, the center-of-mass motion of the cluster is calculated. Second, the radial and

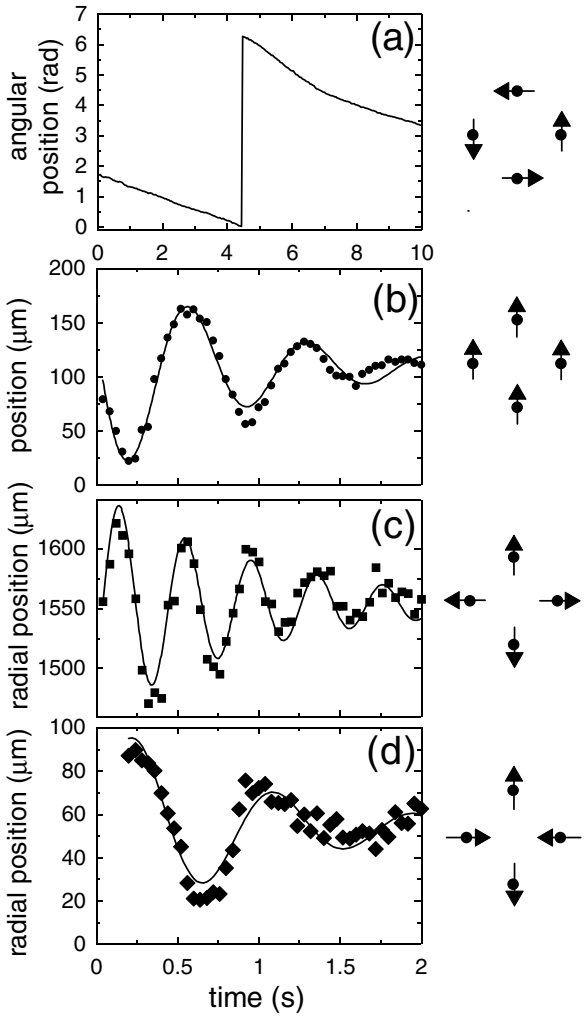

FIG. 2. Normal modes of the $N = 4$ cluster. (a) rotation around the center of the potential well, (b) center-of-mass motion, (c) breathing mode, (d) antisymmetric mode. The symbols denote experimental values. The lines are best fits of damped oscillations to the experimental data.

TABLE I. Experimentally determined values of the mode frequencies ω in $1/s$ for the different clusters. The error range is the standard deviation from the analysis of 10 to 20 different excitations.

N	Center-of-mass ω_0	Breathing ω_{br}	Antisymmetric ω_{as}
3	7.50 ± 0.14	15.42 ± 0.10	···
4	7.91 ± 0.13	16.14 ± 0.10	6.93 ± 0.45
7	7.60 ± 0.17	15.82 ± 0.06	9.66 ± 0.43

angular positions of all particles in the cluster are determined with respect to the center-of-mass. The breathing mode is then obtained as the oscillation of the sum of the radial positions $\sum r_i/N$. Finally, the antisymmetric mode is determined from the alternating sum, i.e., $(r_1 - r_2 + r_3 - r_4)/4$ when using the $N = 4$ cluster as an illustrative example.

The measured oscillations are shown in Fig. 2 for the $N = 4$ cluster. In Fig. 2(a), the nonoscillatory ($\omega = 0$) rotation around the center of the potential well is shown for 10 s. The center-of-mass motion [Fig. 2(b)], the breathing mode [Fig. 2(c)], and the antisymmetric mode [Fig. 2(d)] are presented over a time of 2s. The modes exhibit a damped harmonic oscillation at frequencies of the order of 1 to 2 Hz. The oscillation frequencies and damping constants are derived by a best fit of a damped harmonic oscillation. The measured frequencies of the normal modes for the center-of-mass motion ω_0, for the breathing mode ω_{br}, and for the antisymmetric mode ω_{as} are listed in Table I for the clusters of 3, 4, and 7 particles. Because of the odd number of particles in the ring the $N = 3$ cluster does not exhibit an antisymmetric mode.

The frequencies of the breathing ω_{br} and the antisymmetric ω_{as} mode have been calculated as a function of screening strength κ from Eq. (6). The normalized frequencies, i.e., $\omega_{\mathrm{br}}^2/\omega_0^2$ and $\omega_{\mathrm{as}}^2/\omega_0^2$, are shown in Figs. 3 and 4 for the $N = 4$ and the $N = 7$ particle clusters, respectively. The curves for the breathing mode are very similar for both clusters. As expected, the frequency of the breathing mode starts at $\omega_{\mathrm{br}}^2/\omega_0^2 = 3$ for pure Coulomb interaction ($\kappa = 0$). Then, the mode frequency increases with screening strength. This counterintuitive result can be understood as follows. With increasing κ, the radial position r_i of the microspheres in the horizontal confinement well is reduced, the clusters become smaller due to the reduced Coulomb repulsion (see Fig. 5). With reduced distance, the curvature of the Debye-Hückel potential increases more strongly than the force, i.e., $r\partial^2\phi/\partial r^2 > 2\partial\phi/\partial r$, which in turn leads to the observed increase of the mode frequency. The size reduction is accompanied by an increase of potential energy with respect to the Coulomb energy (see Fig. 5). In a simplified picture, this means that under the "pressure" of the confinement the particles are pushed into regions with steeper curvature of the interaction potential.

The frequency of the antisymmetric mode shows a different behavior for different cluster sizes ($N = 4$ and 7).

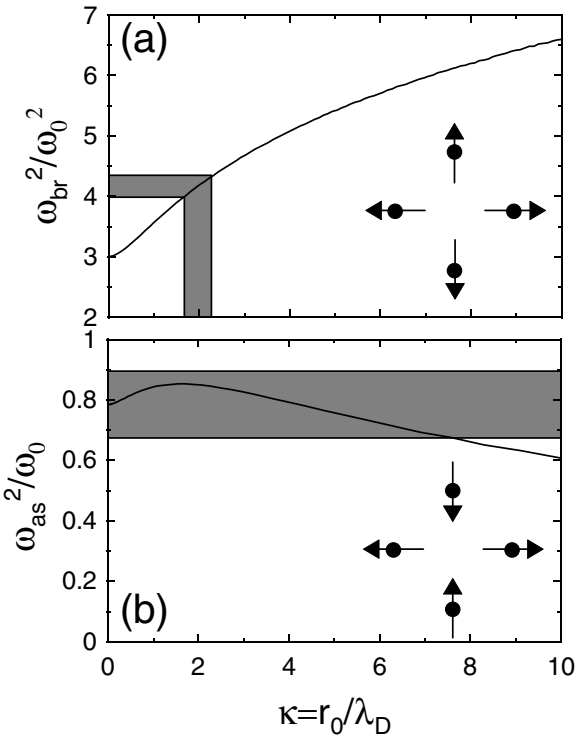

FIG. 3. Normalized frequencies of (a) the breathing mode and (b) the antisymmetric mode of the $N = 4$ cluster as a function of κ. The shaded areas correspond to the measured values of $\omega_{\mathrm{br}}^2/\omega_0^2$ and $\omega_{\mathrm{as}}^2/\omega_0^2$.

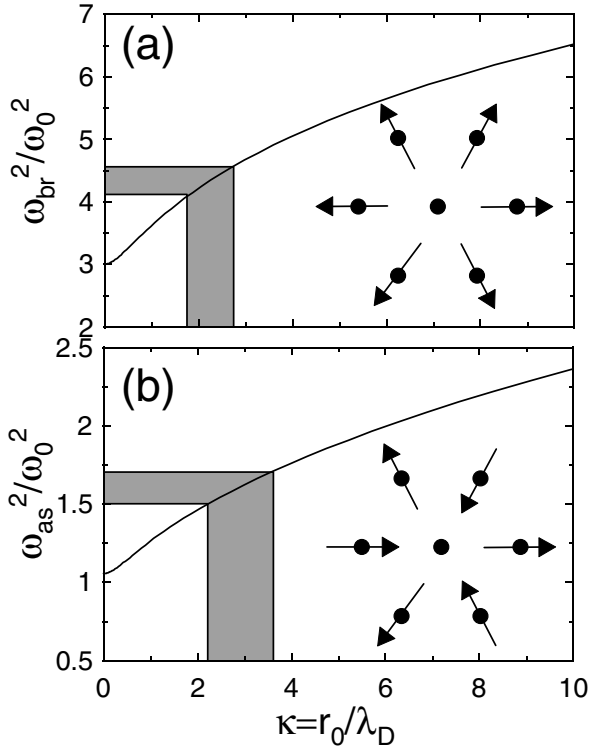

FIG. 4. Normalized frequencies of (a) the breathing mode and (b) the antisymmetric mode of the $N = 7$ cluster as a function of κ. The shaded areas correspond to the measured values of $\omega_{\mathrm{br}}^2/\omega_0^2$ and $\omega_{\mathrm{as}}^2/\omega_0^2$.

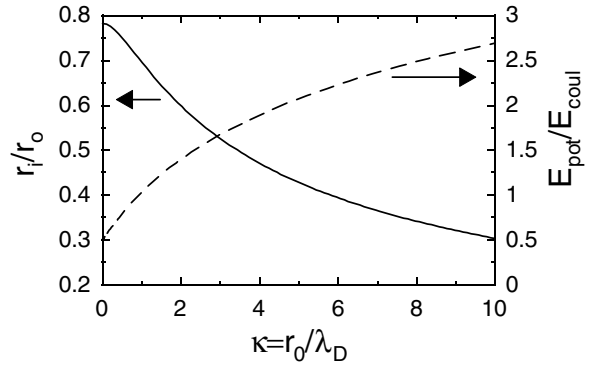

FIG. 5. (a) Normalized particle positions in the confining well (solid line) and Coulomb energy over potential energy (dashed) as a function of κ for a $N = 4$ cluster.

For the $N = 4$ cluster, the mode frequency has only a weak dependence on the screening strength, whereas for the $N = 7$ cluster the antisymmetric mode frequency increases with screening strength in a similar way as the breathing mode. This different behavior can be attributed to the presence of the central particle in the case of the $N = 7$ cluster which makes the antisymmetric mode stiffer.

By comparison of the measured values of the frequencies of breathing and antisymmetric mode with the theoretical curves the screening strength κ has been derived for the different clusters; see Figs. 3 and 4. The obtained values for κ are listed in Table II. From the breathing mode a screening strength of $\kappa = 2.1 \pm 0.4$ is a consistent result for all clusters. Using the normalization to the particle distances $\kappa' = r_i/\lambda_D$ the screening strength is found to be $\kappa' = 1.05 \pm 0.2$ in very good agreement with earlier results obtained by wave experiments in extended 2D systems [15,16,18]. From the antisymmetric mode the screening strength is derived with less accuracy. For the 4-particle cluster the entire range of $\kappa < 7.5$ is compatible with the observations. The value for κ derived from the $N = 7$ cluster is somewhat larger than that from the breathing mode, but the error ranges overlap.

Since from the experiments all quantities (ω_0, all particle positions and interparticle distances r_i, r_{ij}, as well as the screening strength κ) are known, the particle charge number Z can also be obtained. In doing so, one has to consider that κ and Z are related through Eqs. (3) and (5). The charge numbers are listed in Table II using the values from the breathing mode. They are found to be centered around $Z = 18\,000$ with an overall error range of 6000 elementary charges. This charge value compares very well with those obtained from collision experiments under similar conditions [17].

In conclusion, 2D finite clusters in complex plasmas provide a unique system to excite and to study weakly damped normal modes in bounded systems of charged particles. From the complex oscillations in finite clusters the normal modes have been extracted. By comparison of measured and calculated frequency ratios of different modes the key parameters, i.e., the confinement frequency ω_0, the screening strength κ, and the particle charge Z have been derived. The close agreement with the results from laser excited waves in plasma crystals demonstrates the accuracy and reproducibility that is now achieved for the charge and screening of the microspheres in a complex plasma. The results from normal modes in 2D are promising for extending this technique to 3D clusters that form under microgravity. There, normal-mode analysis will be one of the key diagnostics for determining the particle charge and shielding effects.

TABLE II. Values of the screening strength κ and the particle charge Z for the different clusters derived from the measured mode frequencies.

N	Breathing mode	Antisymmetric mode	Breathing mode
3	$\kappa = 2.17 \pm 0.4$	⋯	$Z = 14\,500 \pm 1500$
4	$\kappa = 1.98 \pm 0.3$	$\kappa < 7.5$	$Z = 17\,000 \pm 2700$
7	$\kappa = 2.25 \pm 0.5$	$\kappa = 2.92 \pm 0.7$	$Z = 22\,200 \pm 5500$

This work was supported by DFG under Contract No. Pi185-17/1 and by INTAS 97-775. The authors are indebted to their late colleague and friend Vitaly Schweigert, whose theoretical investigations were stimulating for this work.

[1] J. J. Thomson, Philos. Mag. **39**, 236 (1904).
[2] D. J. Wineland *et al.,* Phys. Rev. Lett. **59**, 2935 (1987).
[3] F. Diedrich *et al.,* Phys. Rev. Lett. **59**, 2931 (1987).
[4] P. Leiderer, W. Ebner, and V. B. Shikin, Surf. Sci. **113**, 405 (1982).
[5] *Nanostructure Physics and Fabrication,* edited by M. A. Reed and W. Kirk (Academic, Boston, 1989).
[6] J. E. Hug, F. van Swol, and C. F. Zukoski, Langmuir **11**, 111 (1995).
[7] S. Neser, T. Palberg, C. Blechinger, and P. Leiderer, Prog. Colloid Polym. Sci. **104**, 194 (1997).
[8] W.-T. Juan *et al.,* Phys. Rev. E **58**, 6947 (1998).
[9] M. Klindworth, A. Melzer, A. Piel, and V. Schweigert, Phys. Rev. B **61**, 8404 (2000).
[10] T. Trottenberg, A. Melzer, and A. Piel, Plasma Sources Sci. Technol. **4**, 450 (1995).
[11] V. M. Bedanov and F. Peeters, Phys. Rev. B **49**, 2667 (1994).
[12] Y.-J. Lai and L. I, Phys. Rev. E **60**, 4743 (1999).
[13] V. A. Schweigert and F. Peeters, Phys. Rev. B **51**, 7700 (1995).
[14] S. G. Amiranashvili, N. G. Gusein-zade, and V. Tsytovich, Phys. Rev. E **64**, 016407 (2001).
[15] A. Homann *et al.,* Phys. Rev. E **56**, 7138 (1997).
[16] A. Homann, A. Melzer, R. Madani, and A. Piel, Phys. Lett. A **242**, 173 (1998).
[17] U. Konopka, G. Morfill, and L. Ratke, Phys. Rev. Lett. **84**, 891 (2000).
[18] A. Melzer, S. Nunomura, D. Samsonov, and J. Goree, Phys. Rev. E **62**, 4162 (2000).